ANNALS OF GEOPHYSICS, 69, 1, GP109, 2026; doi:10.4401/ag-9365
OPEN ACCESS

Magnetic Inversion under Remanent Conditions Using Equivalent Layer Direction Estimation and VOXI Earth Modelling

Sebastião W. N. Moura[1], Shayane P. Gonzalez[2], Saulo S. Martins[*,1]

(1) Graduate Program in Geophysics, Universidade Federal do Pará, Pará, Brazil
(2) Coordenação de Geofísica, Observatório Nacional, Rio de Janeiro, Brazil

Article history: received May 10, 2025; accepted January 24, 2026

Abstract

Remanent magnetisation is a critical challenge in magnetic interpretation, often leading to mispositioned anomalies and unreliable inversion results when neglected. This study applies and validates a practical, sequential two-step workflow that integrates existing techniques to improve magnetic modelling in scenarios where remanent components significantly influence the anomaly geometry. In the first stage, the total magnetisation direction is estimated using the Equivalent Layer technique, which reconstructs the effective magnetisation vector from the observed anomaly without decomposing it into induced and remanent components. The magnetisation direction estimated via the equivalent layer technique was used to perform the reduction to the pole (RTP), and the inversion was subsequently carried out assuming a vertical inducing field (D = 0°, I = 90°). The methodology was tested on synthetic models with varying remanent contributions to evaluate its performance in controlled conditions. Results demonstrate that incorrect directional assumptions lead to distorted source geometries and underestimated susceptibilities, whereas using the Equivalent Layer estimated direction significantly improves inversion accuracy. The approach was also applied to a real airborne magnetic dataset from Espírito Santo State, Brazil, where it successfully recovered a westward-dipping magnetic body with coherent susceptibility structure. Residual analysis confirmed strong agreement between predicted and observed fields, reinforcing the method's robustness. While the current implementation assumes a constant magnetisation direction within the target volume, making it less suitable for geologically complex bodies, it offers a stable and interpretable solution for cases where remanence is spatially coherent. This study provides a practical, reproducible workflow for the integrated application of EL-based direction estimation, RTP, and VOXI susceptibility inversion to remanence-affected datasets. This workflow is compatible with standard modelling platforms and provides a practical reference for remanence-affected magnetic interpretation.

Keywords: Magnetic; Remanence; Inversion; Equivalent Layer; VOXI

1. Introduction

Magnetometry is a key method in applied geophysics, widely used to map variations in the Earth's magnetic field and to infer the physical properties of subsurface structures. Its effectiveness has been demonstrated in mineral exploration, structural mapping, and environmental studies due to its high resolution and non-invasive nature (Blakely, 1995; Telford et al., 2003; Milsom and Eriksen, 2011).

Despite its broad applicability, remanent magnetisation (magnetism retained in rocks after removal of the inducing field) can significantly hinder the interpretation of magnetic anomalies (Nagata, 1961; Schmidt et al., 2014). In many geological environments, this remanence differs considerably in direction and intensity from the induced magnetisation, especially in low-latitude regions, leading to severe distortions in anomaly shape and amplitude (Brown and McEnroe, 2011; Liu et al., 2020b).

Traditional inversion approaches often assume that the total magnetisation aligns with the present-day geomagnetic field, enabling techniques such as reduction to the pole (RTP) followed by susceptibility inversion (Nabighian, 1984; Li and Oldenburg, 1996). However, this assumption fails in scenarios with significant remanence, leading to unreliable inversion results and incorrect geometric interpretations of the sources (Schmidt et al., 2014; Barbosa, 2021).

To overcome these limitations, recent studies have employed equivalent layer (EL) techniques to estimate the direction of total magnetisation (Reis et al., 2016, 2019; Gonzalez et al., 2020, 2022) following earlier developments that also applied the equivalent-source concept for direction recovery (Nicolosi et al., 2006). This approach replaces real sources with a distribution of planar dipoles and solves for their orientation and magnitude under positivity constraints. The estimated inclination and declination of the magnetisation vector can then be used as input parameters in constrained magnetic inversion workflows, such as those implemented in the VOXI Earth Modelling platform (Li and Oldenburg, 1996; MacLeod et al., 2016).

The integration of these two methodologies – equivalent-layer-based estimation of total magnetisation and constrained-susceptibility inversion – forms a robust workflow that enhances the recovery of magnetised bodies, even in geologically complex environments where conventional RTP fails. Nevertheless, few studies have combined both strategies in a coherent framework, tested using synthetic models, and validated with real data (Gonzalez et al., 2020, 2022).

In this work, we apply and evaluate a two-step magnetic inversion workflow for remanence-dominated environments. First, we estimate the total magnetisation direction using the equivalent layer method under a positivity constraint. Next, we perform a magnetic susceptibility inversion in VOXI using the anomaly reduced to the pole (RTP) with the direction estimated from the equivalent layer, assuming a vertical inducing field ($D = 0°$, $I = 90°$). The methodology is validated through synthetic models that simulate both induced and remanent magnetic conditions and further tested on real magnetic data acquired over the Norite of São Gabriel de Baunilha, located in Espírito Santo, Brazil.

The objective is to assess how the total magnetisation direction estimated by the equivalent layer (inclination and declination) can be used to perform a reduction to the pole (RTP) and generate a magnetically centred anomaly for VOXI inversion under a vertical inducing field. This sequential procedure provides a reproducible and physically consistent framework for recovering the geometry and volume of magnetic bodies in settings dominated by remanent magnetisation.

The estimation of total magnetisation direction using equivalent sources has been previously explored in the literature (e.g., Nicolosi et al., 2006; Reis et al., 2019, 2020; Gonzalez et al., 2020). In this study, these concepts are systematically integrated into a coherent and reproducible workflow that combines equivalent-layer-based direction estimation with conventional magnetic susceptibility inversion, and their performance is evaluated using controlled synthetic models and a real airborne dataset.

2. Theoretical Background

2.1 Total Magnetic Field and Remanence

The total magnetic anomaly recorded in a survey results from the vector sum of the induced and remanent magnetisation of subsurface materials. Remanent magnetisation may include thermoremanent, depositional, or

chemical components, depending on the geological setting (Nagata, 1961; Schmidt et al., 2014). In many rock types – especially those rich in ferromagnetic minerals – remanent magnetisation can exceed the induced component and be oriented in a direction significantly different from the induced component (Brown and McEnroe, 2011; Liu et al., 2020a).

This vectorial discrepancy complicates the interpretation of magnetic anomalies and poses a challenge to conventional geophysical workflows, particularly when the remnant component dominates the total magnetisation. Accurate estimation of the magnetisation direction becomes essential to ensure reliable interpretation and inversion results (Dentith and Mudge, 2014).

2.2 Reduction to the Pole and Its Limitations

Reduction to the pole (RTP) is one of the most widely used transformations in magnetic data interpretation. It assumes that the source magnetisation is aligned with the present-day geomagnetic field, allowing anomalies to be repositioned directly over their causative bodies (Blakely, 1995; Reeves, 2005). This approach is effective in high-latitude regions or when remanent magnetisation is negligible.

However, when the total magnetisation differs significantly from the geomagnetic field – due to a strong remanent component – RTP can introduce artefacts such as amplitude asymmetry, lateral displacement of anomalies, and spatial distortion of sources (Li, 2008; Luo and Wu, 2023). These issues are particularly severe at low magnetic latitudes, where the Earth's field is nearly horizontal and RTP becomes numerically unstable (Melo et al., 2021; Jian et al., 2022).

Alternative methodologies have been developed to address these limitations. Among them are approaches based on analytic signal fitting, vector magnetisation inversion, and equivalent layer techniques, which aim to estimate the true direction of total magnetisation before applying inversion procedures (Li and Oldenburg, 2001; Li et al., 2010; Reis et al., 2019, 2020; Gonzalez et al., 2020, 2022). In this study, we adopt the equivalent layer method constrained by positivity, which enables the estimation of the magnetisation direction directly from gridded magnetic data.

2.3 Equivalent Layer Technique

The equivalent layer (EL) technique replaces real magnetic sources with a planar dipole distribution at a constant depth. These equivalent sources are adjusted to reproduce the observed magnetic field at the surface, allowing flexible modelling and robust interpretation of magnetic anomalies (Dampney, 1969; Reis et al., 2019, 2020).

When the dipole moments are constrained to be positive, the EL method can be used to estimate the total magnetisation direction that best fits the observed anomaly, even in the presence of strong remanent components (Reis et al., 2019; Gonzalez et al., 2020; Reis et al., 2020). This estimation is based on a trial-and-error approach, where the magnetisation direction is iteratively varied until the best agreement between observed and modelled data is achieved, subject to the positivity constraint.

Mathematically, the predicted anomaly at an observation point p_i is given by:

$$\Delta Ti = \sum_{j=1}^{M} m_j a_{ij}\left(\hat{f}, \hat{s}\right) \tag{1}$$

where m_j is the magnetic moment of the j-th dipole, and $a_{ij}(\hat{f}, \hat{s})$ is a sensitivity function that depends on the direction of the geomagnetic field ($\hat{f}$) and the assumed total magnetisation vector ($\hat{s}$), the total number of dipoles in the layer is M.

By minimising the misfit between observed and calculated data and ensuring the positivity of all m_j, the total magnetisation direction (I_S, D_S) most accurately represents the true source distribution, which can be recovered. This technique has proven effective in estimating total magnetisation direction from aeromagnetic data without requiring direct rock sampling (Gonzalez et al., 2022).

However, the reliability of this method depends on key assumptions. All real sources should lie beneath the equivalent layer, and the estimated direction should represent a uniform total magnetisation (Reis et al., 2020). Violating these assumptions may reduce accuracy or lead to instability in the inversion results. Nevertheless, the technique remains a powerful tool for magnetisation direction estimation in remanence-dominated environments.

2.4 Magnetic Susceptibility Inversion

Magnetic susceptibility inversion aims to estimate the spatial distribution of magnetic sources in the subsurface by adjusting a 3-D model to fit observed total field anomalies. It is a widely used method in aeromagnetic interpretation, providing insights into the geometry, depth, and contrast of buried structures (Reeves, 2005; Li and Oldenburg, 1996).

The inversion process is inherently ill-posed, meaning that minor data uncertainties can result in significant variations in the model. To mitigate this, stabilisation techniques such as Tikhonov regularisation or minimum gradient support are commonly applied (Tikhonov, 1963; Barbosa and Silva, 1994). In this context, each model grid cell is assigned a magnetic susceptibility value, and inversion algorithms adjust these values to minimise the misfit between observed and predicted data (Li and Oldenburg, 1996; Pilkington, 1997).

In this study, the susceptibility inversion was performed using the VOXI Earth Modelling platform. Although the full implementation is proprietary, the inversion follows classical magnetic inversion approaches based on regularisation and iterative reweighting, similar to those introduced by the UBC-GIF group (Li and Oldenburg, 1996). Additionally, concepts such as cut-cell techniques and model focusing align with the developments described by Ingram et al. (2003).

To improve the inversion's robustness, the direction of magnetisation estimated by the equivalent layer method was incorporated as a fixed input. This allows the inversion to account for remanent magnetisation, avoiding errors typically introduced when assuming induced magnetisation aligned with the geomagnetic field.

To improve the inversion's robustness, the direction of magnetisation estimated by the equivalent-layer method was used to compute the reduction-to-pole (RTP) of the observed total-field anomaly. The susceptibility inversion in VOXI was then performed on this RTP-transformed dataset, assuming a vertical inducing field ($D = 0°$, $I = 90°$). In this configuration, the effects of remanent magnetisation are handled in the RTP pre-processing step, while the inversion itself adopts the standard vertical-field formulation.

The inversion was conducted on a 3-D mesh with 10 m cell resolution, constrained by a digital elevation model (DEM) and using iterative reweighting (IRI) to sharpen susceptibility contrasts. Regularisation parameters were calibrated to balance model smoothness and geological realism, with isotropic gradient weighting and positivity constraints enforced throughout (Cunningham et al., 2021; Guevara-Betancourt et al., 2023).

This combined approach enables the recovery of geometrically realistic and geophysically consistent models, even in complex geological environments where traditional RTP-based workflows would fail.

3. Methodology

The proposed workflow addresses the limitations of conventional magnetic inversion methods in remanent magnetisation. It integrates equivalent-layer processing and 3-D magnetic-susceptibility inversion into a sequential strategy to improve recovery of source geometry and volume. The procedure consists of four main steps:

1) Construction of synthetic models simulating different magnetisation scenarios, including: (i) induced magnetisation, (ii) misestimated total magnetisation, and (iii) corrected total magnetisation;
2) Estimation of the total magnetisation direction using the equivalent layer method under positivity constraints;
3) Application of 3-D magnetic susceptibility inversion using the VOXI Earth Modelling system on the anomaly reduced to the pole (RTP) with the direction estimated from the equivalent layer;
4) Validation of the methodology through comparison with synthetic models and application to real aeromagnetic data.

This integrated strategy is designed to generate geologically realistic models in scenarios where traditional reduction to the pole (RTP) and induced-only assumptions fail due to the influence of remanent magnetisation.

3.1 Synthetic Model Design

To evaluate the proposed approach under controlled conditions, synthetic magnetic anomalies were generated using a spherical source embedded in a homogeneous, non-magnetic medium. Forward modelling was performed using the open-source SimPEG framework (Cockett et al., 2015).

The synthetic source is a sphere with a radius of 200 m, centred at a depth of 250 m. The magnetic susceptibility of the sphere is set to $\chi = 0.1$ SI, and the background is assigned a value of 10-4 SI. The total magnetic anomaly was simulated using a geomagnetic field with inclination I = −34°, declination D = −23°, and field intensity of 24,000 nT.

Three distinct magnetisation scenarios were tested:

- Model A (Induced only): Total magnetisation aligned with the geomagnetic field;
- Model B (Incorrect direction): True total magnetisation with I = −48°, D = −68°, but RTP and inversion assume induced-only direction;
- Model C (Direction corrected via EL): Same as Model B but using the total magnetisation direction estimated with the equivalent layer technique prior to inversion.

In all synthetic cases, a structured mesh composed of 20 m cubic cells was used to ensure complete containment of the source. Gaussian noise corresponding to 2% of the total anomaly amplitude was added to simulate realistic acquisition conditions.

3.2 Real Data Acquisition and Preprocessing

The real magnetic data used in this study were obtained from the Espírito Santo airborne geophysical survey conducted by the Geological Survey of Brazil (SGB-CPRM). The survey covered the Norite of São Gabriel de Baunilha (NSGB), a mafic intrusive unit within the Araçuaí Orogen, located in Santa Maria de Jetibá, Espírito Santo.

Measurements were acquired using fixed-wing aircraft equipped with caesium-vapour magnetometers in a stinger configuration. Data were sampled at 0.1 s intervals, resulting in an average point spacing of 7.7 m along the flight lines. The flight plan included north-south lines spaced 500 m apart and east-west tie-lines spaced 5,000 m, flown approximately 100 m above ground level. The dataset corresponds to map sheet 1093 and is publicly available through the GeoSGB platform[1].

Preprocessing followed the standard SGB workflow, including diurnal correction, IGRF subtraction, lag correction, heading correction, and statistical levelling. Microlevelling was applied using a directional polynomial filter to suppress residual line-level artefacts.

Initial RTP transformation revealed persistent bipolar anomalies, suggesting that remanent magnetisation significantly affects the NSGB. This observation motivated the adoption of the equivalent layer-based magnetisation estimation and constrained inversion approach applied in this study.

3.3 Inversion Parameters and Constraints

Magnetic susceptibility inversion was performed separately for synthetic (modelled) and real datasets, each with configurations tailored to their respective conditions. Both inversions employed isotropic regularisation and positivity constraints on susceptibility values.

For the synthetic datasets, inversions were performed on a regular mesh with cell dimensions of 100 × 100 × 50 m. The magnetisation direction varied according to each scenario as follows:

- Model A (Induced only): magnetisation aligned with the geomagnetic field (IGRF).
- Model B (Incorrect direction): The True total magnetisation direction is misrepresented by assuming the induced field (IGRF).
- Model C (Direction corrected via EL): Total magnetisation direction accurately estimated via the equivalent layer method.

Gradient weighting was uniform in all directions, and iterative reweighting inversion (IRI) was applied to enhance boundary contrast. Table 1 (Synthetic and Real Data) summarises the inversion constraints and parameters.

The real aeromagnetic dataset was inverted using the VOXI Earth Modelling platform. Consistent with the input data resolution, a 3D mesh with cell dimensions of 100 × 100 × 50 m, was adopted. The digital elevation model (DEM)

1 GeoSGB Platform: https://geosgb.sgb.gov.br/.

defined the surface boundary. The magnetisation direction estimated via the equivalent layer technique was used to perform the reduction to the pole (RTP), and the inversion was subsequently carried out assuming a vertical inducing field (D = 0°, I = 90°).

Table 1. VOXI inversion constraints and parameters for synthetic and real datasets.

Parameter	Synthetic Data	Real Data
Cell size	100 × 100 × 50 m	250 × 250 × 125 m
Mesh dimensions (cells)	42 × 42 × 18	56 × 34 × 19
Geomagnetic field intensity	24,000 nT	23,886 nT
Inclination	90°	90°
Declination	0°	0°
Background trend (constant)	0.37245 nT	48.52769 nT
Absolute fit error (nT)	0.4666 nT	10.85 nT
Gradient weighting (EW, NS, Vertical)	1 / 1 / 1	1 / 1 / 1
Parameter weighting	0.0001	0.0001
Edge sharpening	Both ends	Both ends
IRI focus factor	2	2
Active model cells	Enabled	Enabled
Reweighting model	Enabled	Enabled
Susceptibility constraint	Positive	Positive

These parameters ensured consistent, robust inversion results, enabling precise validation of the methodology in both synthetic and real-world scenarios.

4. Synthetic Tests

A series of synthetic tests was performed to validate the proposed methodology. These tests aimed to evaluate the workflow's performance under different magnetisation conditions, all in the presence of noise. Three cases were analysed: (i) a model with purely induced magnetisation, (ii) a model with combined induced and remanent magnetisation but using an incorrect magnetisation direction (assumed induced), and (iii) a model with combined induced and remanent magnetisation where the total magnetisation direction was estimated using the equivalent layer technique. For each case, the magnetic anomaly, the reduction to the pole, the predicted data from the inversion, and the residuals were examined. Finally, the results were compared to assess the influence of directional assumptions and the benefits of the proposed correction strategy.

4.1 Case A: Induced magnetisation only

In the first synthetic test, we considered a sphere-shaped body magnetised solely by the induced field, under a noisy scenario. The observed total magnetic field anomaly, its RTP, the modelled data after inversion, and the residuals are shown in Fig. 1.

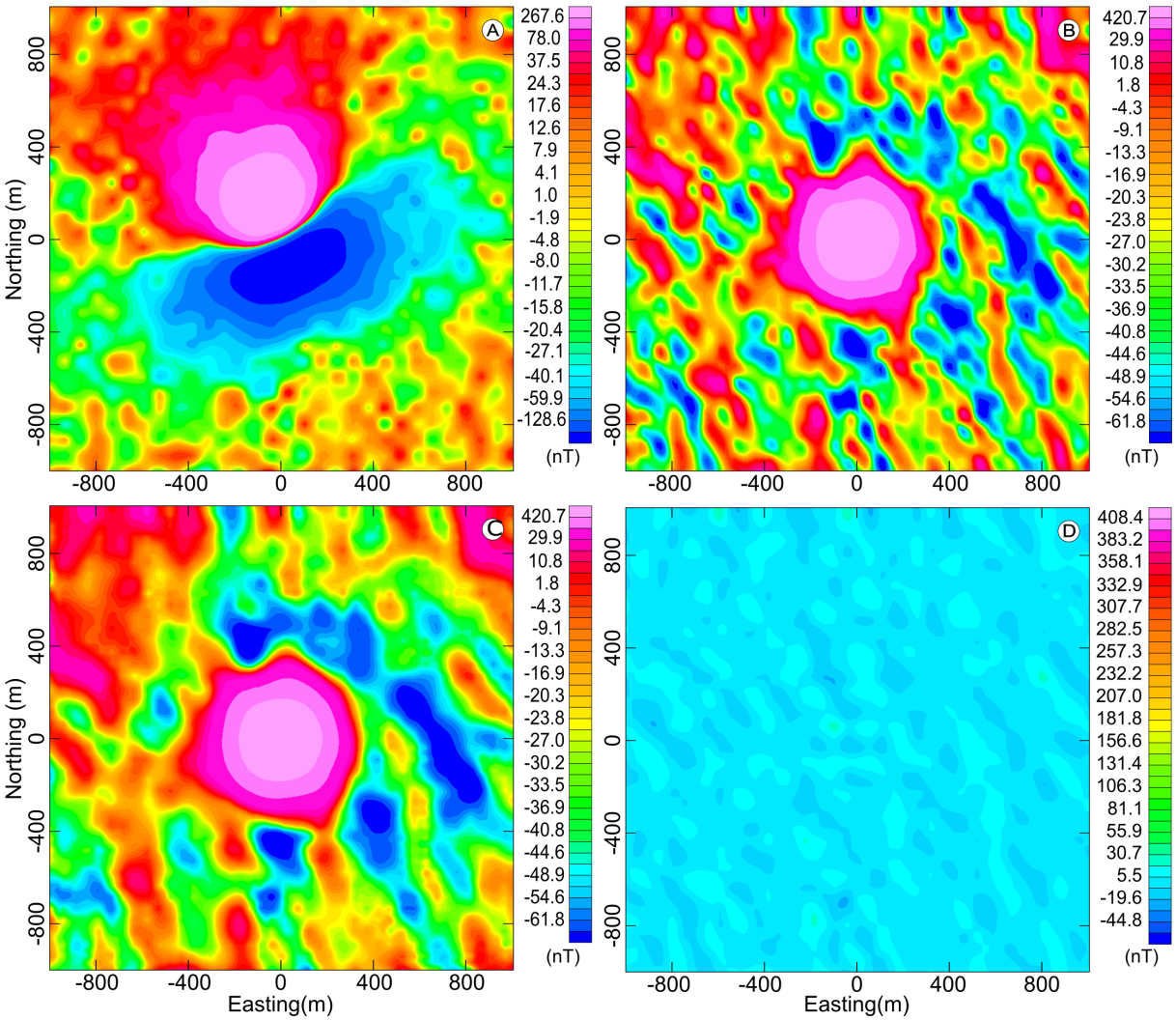

Figure 1. Synthetic Test Case A: (A) Observed Total Magnetic Field Anomaly; (B) Reduction to the Pole; (C) Predicted Data after Inversion; (D) Residuals.

The RTP process correctly centred the anomaly over the source body, enabling an accurate geometry recovery through the susceptibility inversion. The residuals were minimal, indicating an excellent fit between the observed and predicted data.

4.2 Case B: Induced + Remanent magnetisation with Incorrect Total Direction

The second test incorporated a remanent magnetisation component distinct from the present geomagnetic field. The RTP assumed only the induced field parameters in this case, ignoring the remanent contribution. Figure 2 presents the magnetic anomaly maps and inversion results.

Due to the incorrect assumption of the magnetisation direction, the RTP failed to centre the anomaly accurately. Nevertheless, the inversion algorithm fit the observed magnetic field reasonably well, as reflected by the predicted data and residuals. The implications for the recovered source geometry are further discussed in Section 4.4.

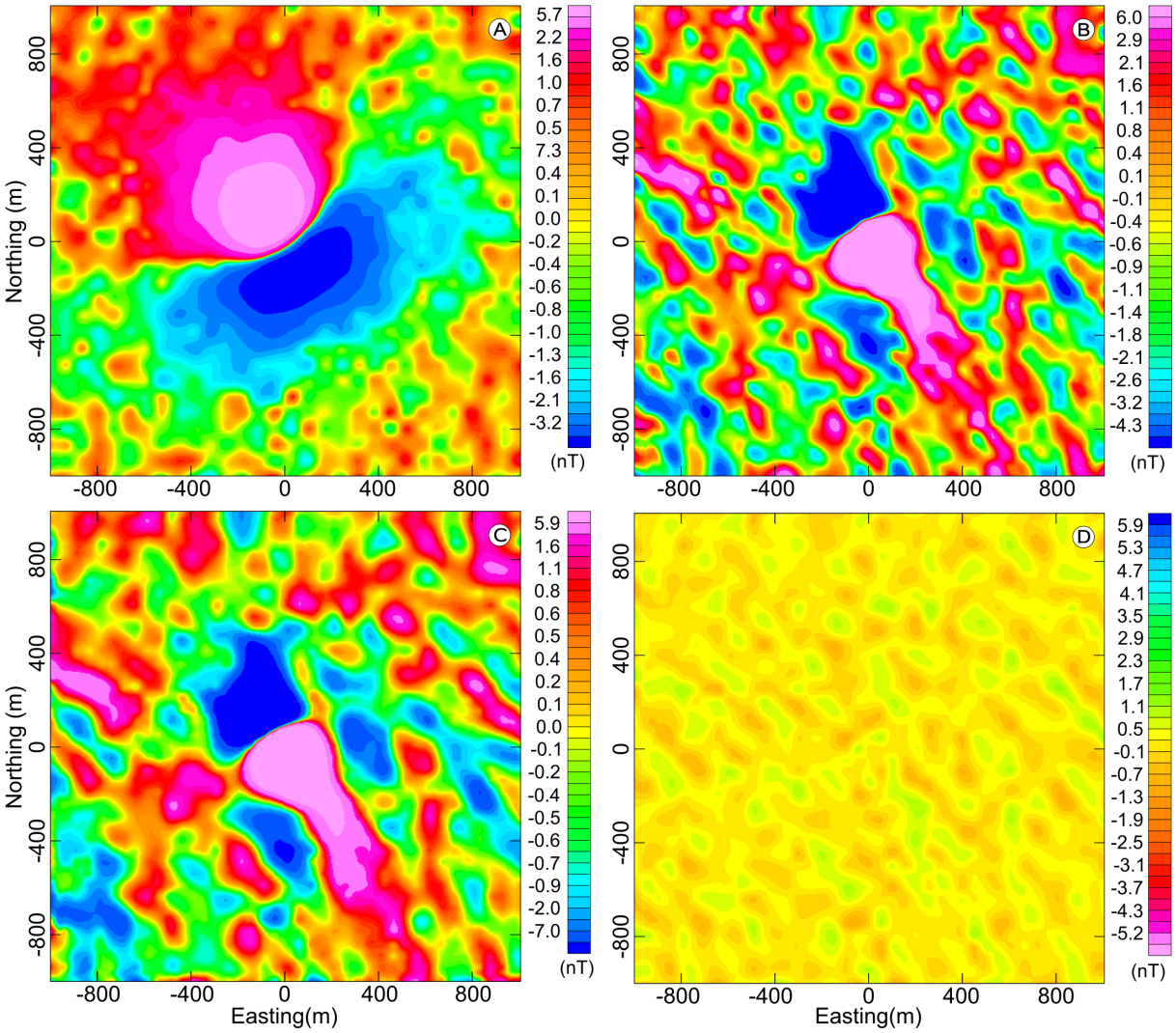

Figure 2. Synthetic Test Case B: (A) Observed Total Magnetic Field Anomaly; (B) Reduction to the Pole assuming induced field; (C) Predicted Data after Inversion; (D) Residuals.

4.3 Case C: Induced + Remanent magnetisation with Estimated Total Direction

The third synthetic test applied the equivalent layer method to estimate the total magnetisation direction before performing RTP and inversion. Figure 3 displays the results obtained.

After estimating the total magnetisation direction, the RTP successfully repositioned the magnetic anomaly over the source. The inversion algorithm produced a predicted field that closely matched the observed anomaly, with substantially lower residuals than in Case B. The assessment of the recovered source geometry is presented in Section 4.4.

These results demonstrate the potential of integrating equivalent layer-based direction estimation with susceptibility inversion to enhance magnetic interpretation in areas affected by strong remanent magnetisation (Reis et al., 2019; Gonzalez et al., 2020). Motivated by the outcomes of the synthetic tests, the proposed methodology is applied to a real magnetic dataset in the following section to further evaluate its practical applicability and effectiveness.

4.4 Comparison of Recovered Models

The final comparison among the three synthetic cases highlights the importance of accurately estimating the magnetisation direction when remanent magnetisation is present. Figure 4 shows the recovered geometries for

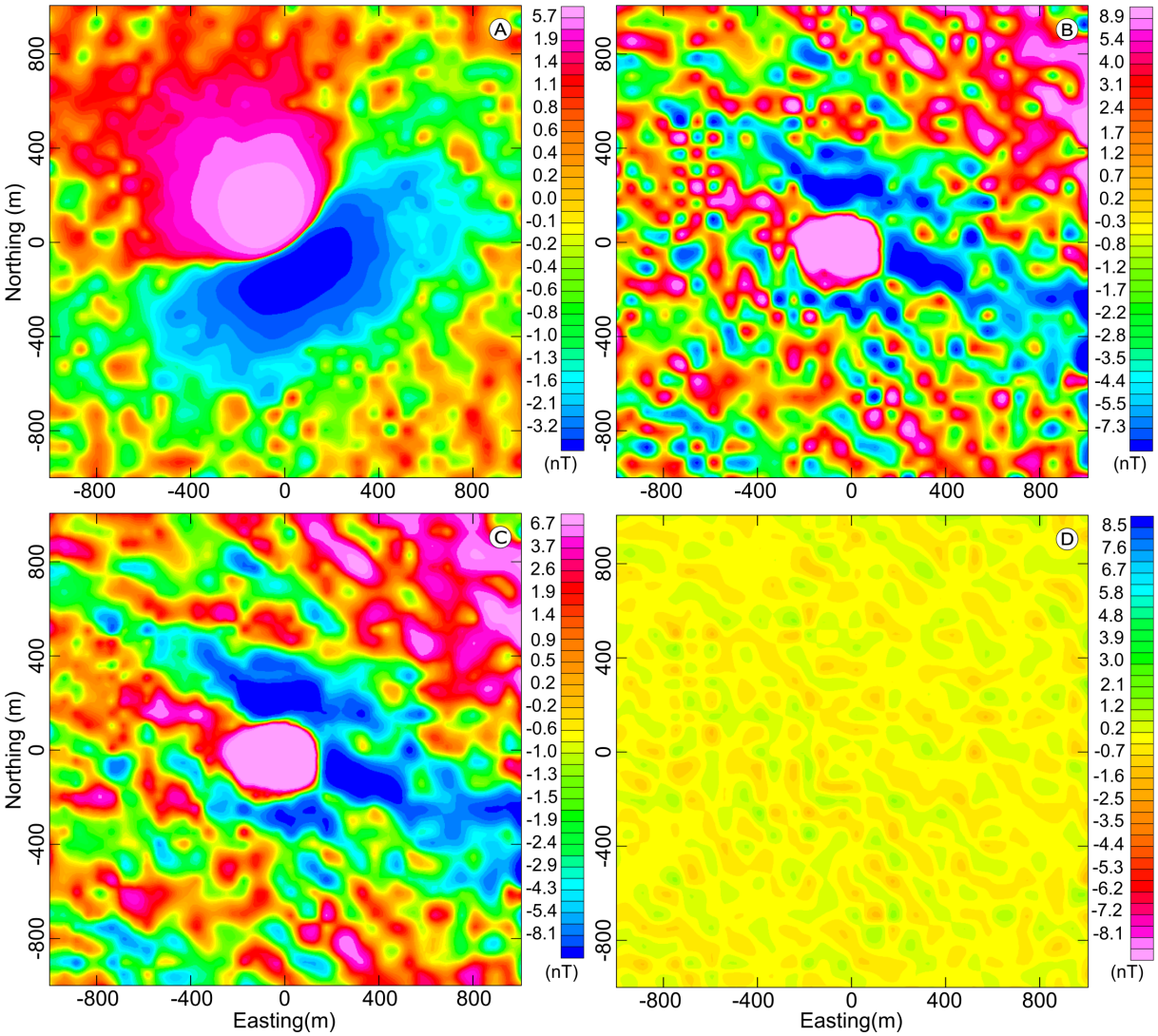

Figure 3. Synthetic Test Case C: (A) Observed Total Magnetic Field Anomaly; (B) Reduction to the Pole after direction estimation; (C) Predicted Data after Inversion; (D) Residuals.

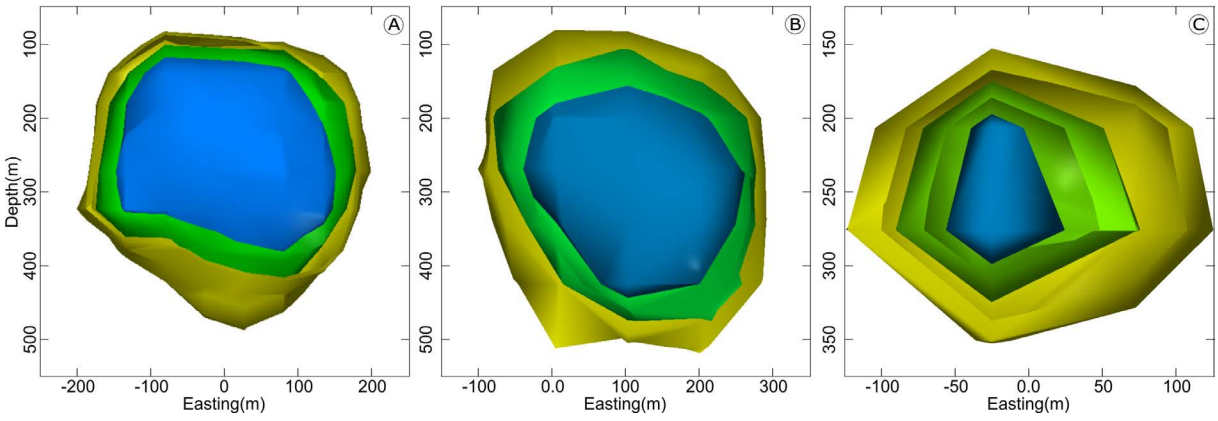

Figure 4. Recovered geometries for Cases A, B, and C. The models were clipped to susceptibility ranges to highlight variation in recovered volumes. The susceptibility thresholds for Cases A and C were 0.15, 0.10, and 0.05; for Case B, they were 0.015, 0.010, and 0.005. Blue volumes correspond to higher susceptibilities and yellow volumes to lower ones.

each scenario. It is important to note that the models were clipped into three susceptibility ranges (represented by the blue, green, and yellow layers) to better visualise the variation in magnetic susceptibility and its effect on the recovered volume. For Cases A and C, the susceptibility cuts were set at 0.15, 0.10, and 0.05, values close to those assigned in the true model. In contrast, for Case B, the thresholds were 0.015, 0.010, and 0.005, indicating an apparent discrepancy from the expected susceptibility values.

In Case A, the absence of remanence allowed a straightforward interpretation, with the recovered geometry closely matching the true model (Fig. 4A). Additionally, the recovered susceptibility values were approximately 0.1, demonstrating that, for a body without remanence, the susceptibility inversion (VOXI; Li and Oldenburg, 1996) successfully recovered both the geometry and susceptibility, even under smoothness constraints.

Although the inversion fit the magnetic data well in Case B, the incorrect assumption about the magnetisation direction resulted in a mislocated and distorted recovered model (Fig. 4B). Furthermore, the recovered susceptibilities were significantly underestimated by approximately one order of magnitude (10^{-1}). This result highlights that applying the inversion assuming only the inducing field (e.g., IGRF) without correcting for remanence can lead to substantial errors when remanent magnetisation is present.

In Case C, the estimation of the correct magnetisation direction enabled the recovery of a geometry much closer to the original sphere, validating the effectiveness of the proposed workflow (Fig. 4C). Nevertheless, the clipped susceptibility layers (0.15, 0.10, and 0.05) indicate that the recovered body is smaller than the true model's size. Thus, even with accurate magnetisation direction estimation, the recovered source volume was ultimately underestimated.

These results demonstrate the potential of integrating equivalent-layer-based direction estimation with susceptibility inversion to enhance magnetic interpretation in areas affected by strong remanent magnetisation (Reis et al., 2019; Gonzalez et al., 2020). Motivated by the outcomes of the synthetic tests, the proposed methodology is applied to a real magnetic dataset in the following section to further evaluate its practical applicability and effectiveness.

5. Application to Real Data

The proposed methodology is applied to a real magnetic dataset presented in this section to further evaluate its practical applicability and effectiveness. The dataset corresponds to an area in Espírito Santo, south-eastern Brazil, and was obtained from airborne magnetic surveys conducted by the Geological Survey of Brazil (SGB/CPRM). The following subsections describe the geological context, data characteristics, processing steps, and the results obtained through the equivalent layer technique and susceptibility inversion.

5.1 Geological Context

The study area is located in the municipality of Santa Maria de Jetibá, Espírito Santo, within the metamorphic-anatectic core of the Araçuaí Orogen. It comprises several geological units, including the São Gabriel de Baunilha Norite (NSGB), the Jequitibá Tonalites, and the Paraíba do Sul Complex, each reflecting distinct tectonic and magmatic processes (Uhlein et al., 2014; Pedrosa-Soares et al., 2001).

The NSGB, a key unit in the northern part of the study area, consists mainly of norite with minor charnockite. It is characterised by grey-dark colour, fine to medium grain size, and a mineralogical assemblage dominated by plagioclase, orthopyroxene, biotite, and quartz. The absence of foliation and phenocryst lineations suggests a post-collisional magmatic flow associated with late-stage intrusions. The NSGB is correlated with the GS Suite (Almorés Suite), which is described as a late-to-post-collisional type I granitic, charnockitic, enderbitic, noritic, and/or anorthositic intrusion (Uhlein et al., 2014; Pedrosa-Soares et al., 2001).

5.2 Data Description and Pre-processing

The magnetic dataset used in this study was acquired during the airborne geophysical survey of the Espírito Santo State (Fig. 5), specifically from the 1093 project sheet conducted by the Geological Survey of Brazil (SGB/CPRM) (Sordi, 2021). The survey parameters included flight lines 500 metres apart and control lines 5000 metres apart,

oriented along the north-south and east-west directions. The flights were conducted at a constant altitude of approximately 100 metres above ground level, using fixed-wing aircraft equipped with caesium vapour magnetometers mounted in stinger configuration. Positioning was provided by a satellite navigation system (GPS) with a positional accuracy of about 1 metre.

Magnetic data were sampled every 0.1 second, corresponding to an average spatial resolution of approximately 7.7 metres along the flight lines. The dataset used in this study was provided in a pre-processed format, including diurnal corrections, removal of the International Geomagnetic Reference Field (IGRF), and levelling adjustments.

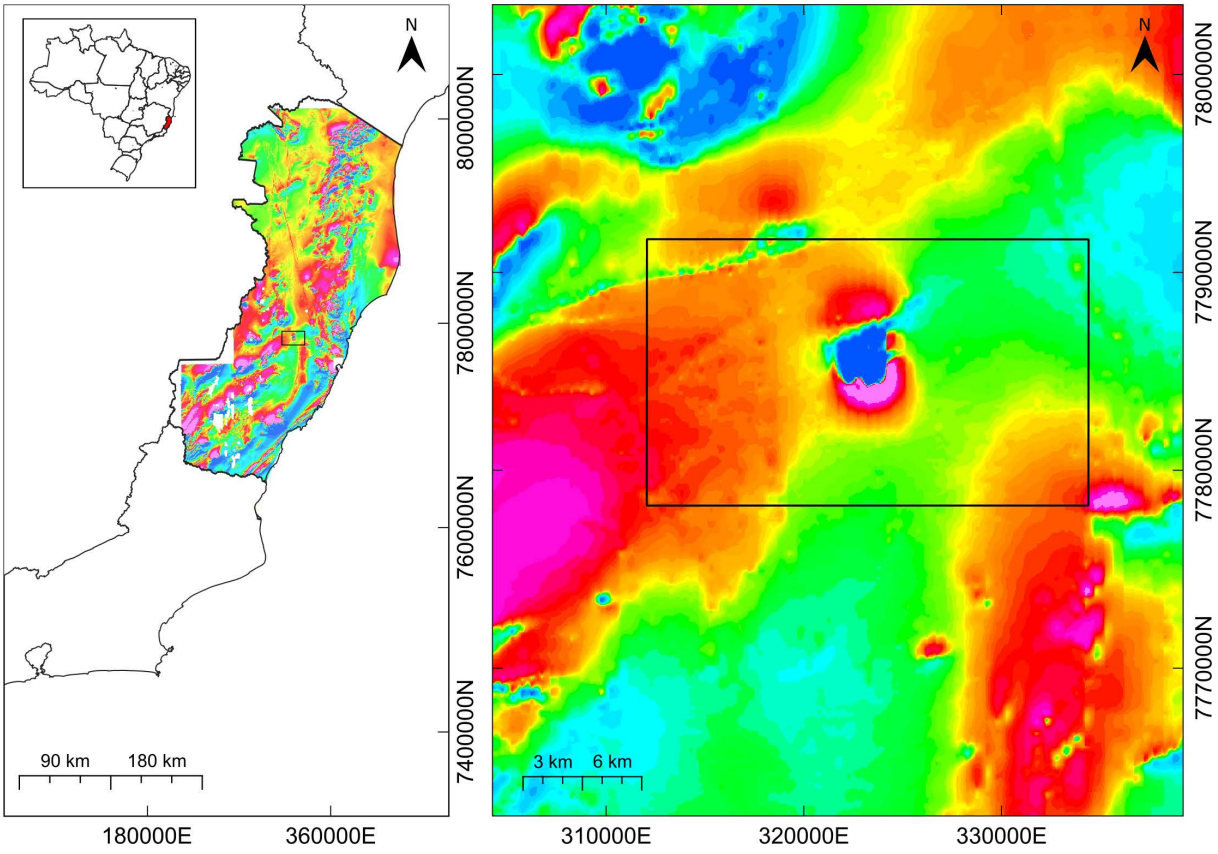

Figure 5. Location of the study area. Left panel: map of Brazil highlighting the Espírito Santo State and selected cartographic sheets from the Geological Survey of Brazil (SGB/CPRM). Right panel: magnetic anomaly map of the selected area used for equivalent layer direction estimation and susceptibility inversion. The highlighted square indicates the subset extracted for detailed analysis. Coordinates are referenced to UTM Zone 24S.

5.3 Estimation of magnetisation Direction

The equivalent layer (EL) technique was applied to estimate the total magnetisation direction from the observed magnetic anomaly, accounting for remanent magnetisation in the study area. Based on the inversion of an equivalent source layer, this method allows the reconstruction of the magnetisation vector without prior assumptions regarding the predominance of induced or remanent components (Reis et al., 2019, 2020; Gonzalez et al., 2020).

In this study, the EL model was discretised over a regular grid with approximately 250 m cell spacing, covering the selected magnetic subset. The layer was positioned at a fixed depth of 150 metres. The actual IGRF parameters for the study area at the time of data acquisition were approximately −23.3° declination and −36° inclination, indicating a non-vertical magnetic field. Therefore, an accurate estimation of the total magnetisation direction was required to perform an effective reduction to the pole (RTP). The inversion was iteratively adjusted to minimise the difference between the observed and calculated anomalies, using a positivity-constrained regularisation approach (Reis et al., 2019).

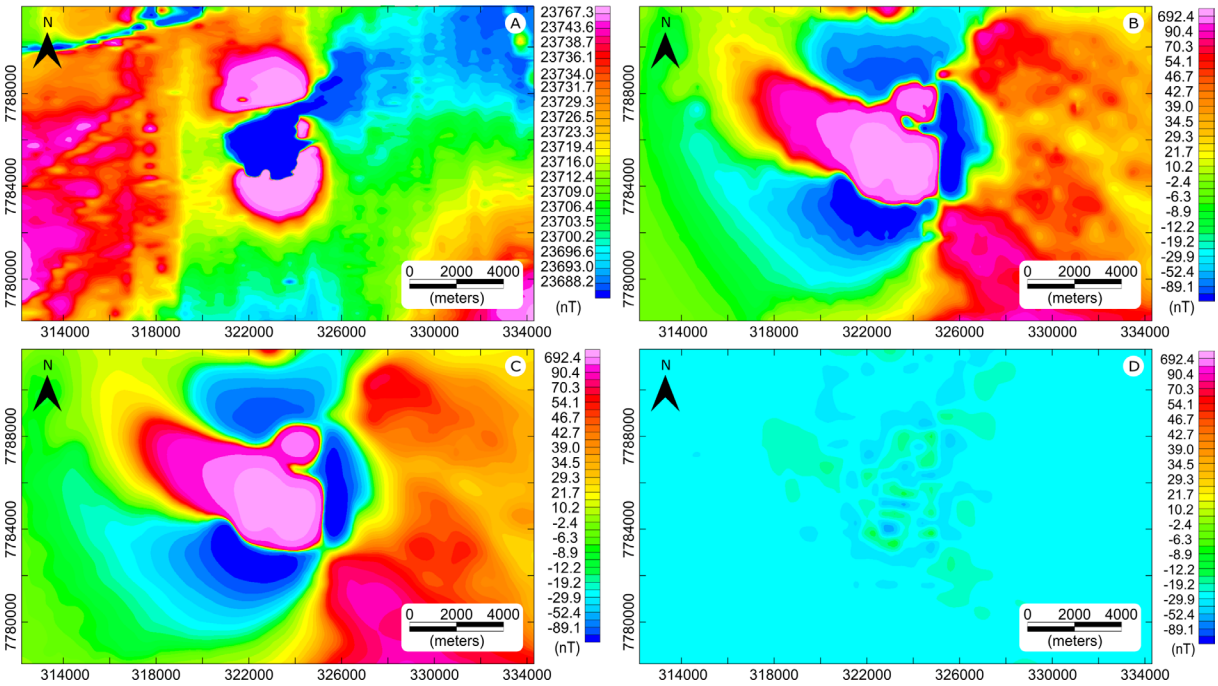

Figure 6. Observed magnetic anomaly used to estimate the magnetisation direction via the equivalent layer method. The anomaly is part of a regional airborne magnetic dataset from the Geological Survey of Brazil (SGB/CPRM) over the Espírito Santo region. The highlighted rectangular subset was selected for inversion, presenting a coherent magnetic response consistent with a remanent magnetic source.

The estimated total magnetisation vector obtained through the EL inversion presented an inclination of 18.56° and a declination of −61.16°. This result indicates that the local magnetic response is strongly influenced by remanent magnetisation, as the estimated direction diverges significantly from the inducing geomagnetic field. The estimated direction was subsequently used in the RTP transformation and served as the input parameter for the susceptibility inversion discussed in the following subsection.

Figure 6 illustrates the observed magnetic anomaly and the results of the equivalent layer inversion used to estimate the magnetisation direction. Panel (A) shows the original observed anomaly. Panel (B) presents the RTP anomaly obtained using the magnetisation direction estimated by the EL method. Panel (C) displays the anomaly predicted by the VOXI inversion, and panel (D) shows the residual between the observed and predicted anomalies. The coherent anomaly pattern and the low residual values support the robustness of the estimated direction, which was subsequently used in the susceptibility inversion.

5.4 Susceptibility Inversion Results

The total magnetic anomaly was transformed using RTP, with the magnetisation direction estimated through the equivalent layer technique (inclination = 18.56°, declination = −61.16°). This corrected dataset was then used as input for the magnetic susceptibility inversion performed using the VOXI Earth Modelling system (Geosoft/Oasis Montaj).

The inversion was configured with a 3-D mesh composed of 250 × 250 × 125 m cells, totalling 56 × 34 × 19 active cells in the X, Y, and Z directions. Padding was applied with five cells horizontally and vertically, and the model's top was positioned at approximately 991 m elevation. The inversion used the magnetic anomaly grid, sampled at a constant altitude of 100 m above the terrain, under the assumption of a vertical inducing field (declination = 0°, inclination = 90°, field strength = 23,707 nT).

A smoothness-constrained inversion was employed with a starting and reference model set to zero, gradient weights of 1.0 in all directions, and a parameter weighting value of 0.0001. The Iterative Reweighting Inversion method was applied with a focus factor of 2, and sharpening was enabled for both ends of the susceptibility distribution. The inversion achieved a final absolute data fit error of approximately 10.85 nT.

The resulting model delineates a moderately elongated, subhorizontal magnetic body at shallow to intermediate depths. The source extends laterally for approximately 3000 metres in the east-west direction and 2000 metres in the north-south direction. Vertically, it spans from about +500 metres down to depths exceeding –2000 metres, resulting in a total thickness greater than 2500 metres. Figure 7 presents the recovered susceptibility distribution, clipped into four intervals (0.05, 0.10, 0.20, and 0.50 SI) to highlight internal variations. These isosurfaces show a central zone of higher susceptibility, surrounded by progressively lower values. While the regularisation may attenuate the absolute susceptibility, the relative contrast is sufficient to support interpreting a coherent magnetic source.

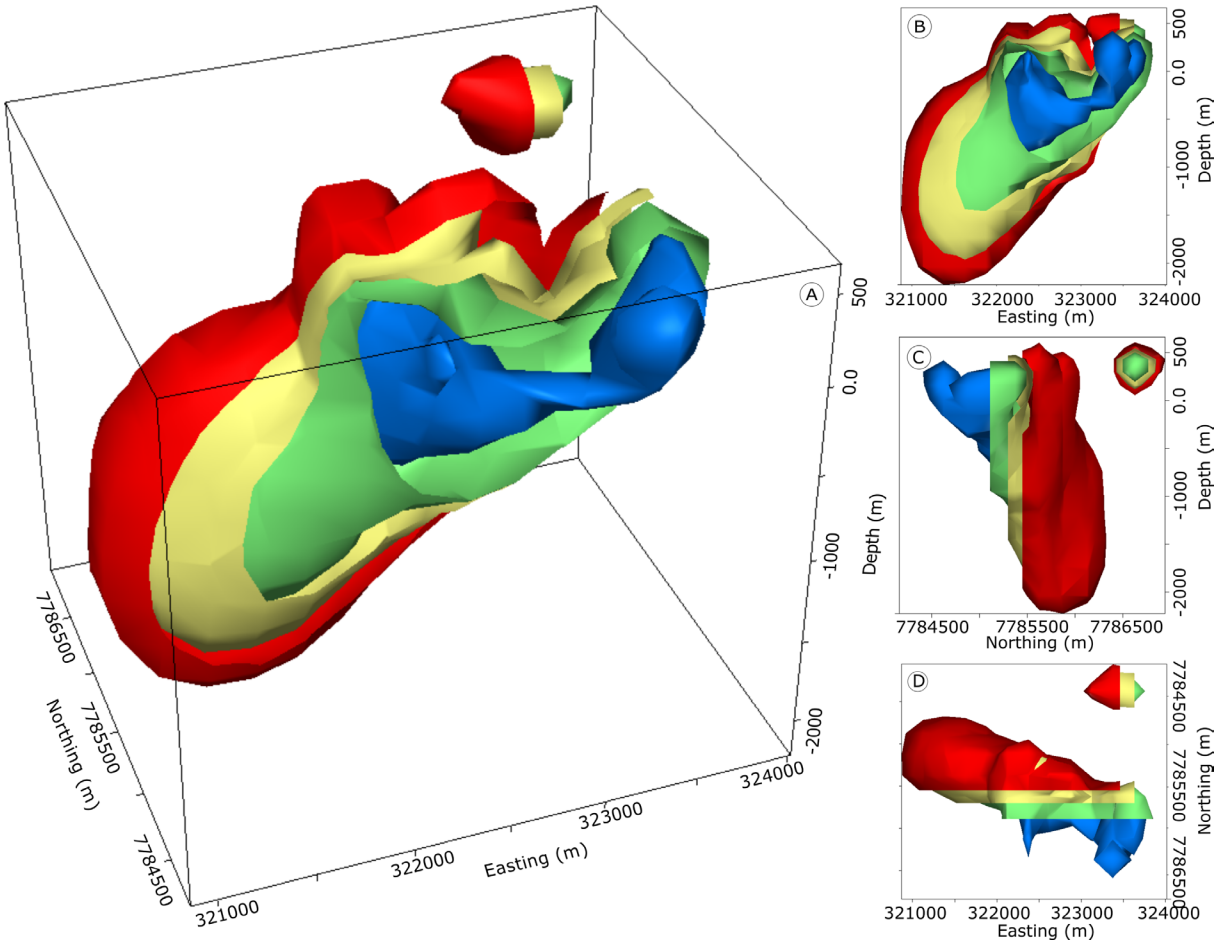

Figure 7. Three-dimensional susceptibility model recovered from the inversion of the RTP-transformed magnetic anomaly. The isosurfaces represent susceptibility thresholds of 0.05, 0.10, 0.20, and 0.50 SI, with red volumes corresponding to the lowest susceptibilities and blue to the highest. (A) Perspective view; (B) East-facing vertical section; (C) North-facing vertical section; (D) Top view showing planimetric distribution of susceptibility.

6. Discussion

The synthetic experiments presented in this study demonstrate the impact of remanent magnetisation on magnetic inversion. In the absence of remanence, conventional susceptibility inversion methods combined with standard reduction to the pole (RTP) are sufficient to recover the geometry and approximate volume of magnetic sources. However, the results are significantly distorted when remanent magnetisation is present and unaccounted for. In such cases, the RTP fails to centre the anomaly correctly, and the resulting inversion produces misleading geometries and severely underestimated susceptibilities. These observations reinforce the need to properly account for the total magnetisation direction, as highlighted by Lelièvre and Oldenburg (2009) and Li et al. (2010).

The main contribution of this study is to demonstrate, through synthetic and real-data examples, how existing techniques can be consistently combined into a practical and robust workflow for handling magnetic data affected

by strong remanent magnetisation. The proposed approach emphasises applied integration and interpretability within a commonly used modelling framework, combining equivalent-layer-based estimation of total magnetisation direction with conventional magnetic susceptibility inversion implemented in the VOXI Earth Modelling system.

The EL approach, as proposed by Reis et al. (2019, 2020), enables the estimation of the magnetisation vector directly from the observed anomaly without assuming the predominance of induced or remanent components. In the proposed workflow, this estimated direction is used to compute a reduction to the pole (RTP) of the total-field anomaly, after which the susceptibility inversion is carried out on the RTP-transformed data under a vertical inducing field (D = 0°, I = 90°). This sequential use of EL-based direction estimation and RTP yields more consistent and interpretable inversion results in both synthetic and real-data applications.

A sensitivity analysis of the equivalent-layer depth and the associated uncertainty of the estimated total magnetisation direction (I, D) are presented in the Appendix. The results confirm that the solution remains stable for shallow layers (100-250 m), with inclination and declination variations within ±1° and ±6°, respectively. These bounds demonstrate the robustness of the EL-based estimation and justify the adopted direction for the RTP correction.

Quantitative metrics for both synthetic and real inversions are summarised in Table 2. The synthetic models (A-C) exhibit consistent recovery of geometry and scale, with volumes ranging from approximately 10×10^6 m^3 to 32×10^6 m^3 and maximum depths between 350 m and 500 m. Model A represents the rounded reference body, Model B a slightly elongated geometry, and Model C a more compact body with a deeper apex. In the real case, the recovered magnetic source reaches depths of approximately 2 km and extends laterally roughly 2 km × 0.6 km, corresponding to an estimated volume of around 8×10^8 m^3. The resulting NE-SW elongation and westward dip agree with field observations and geological mapping of the São Gabriel de Baunilha norite, highlighting the coherence between the geophysical and geological interpretations.

Table 2. Quantitative metrics for synthetic and real inversions.

Case	Data	Cell size (m)	Max depth (m)	Lateral extent (m)	Volume ($\times 10^6$ m^3)
A	Synthetic	100 × 100 × 50	~500	~400 × 400	~32
B	Synthetic	100 × 100 × 50	~500	~350 × 350	~28
C	Synthetic	100 × 100 × 50	~350	~200 × 200	~10
D	Real	250 × 250 × 125	~2000	~2000 × 600	~800

In relation to Li et al. (2010), our contribution is not a new inversion method, but an applied end-to-end workflow in which EL-based direction estimation is used to compute an RTP-transformed dataset, and susceptibility inversion is then carried out on the RTP data under a vertical inducing field. This provides a practical way to reduce directional bias in remanence-affected datasets while remaining within standard modelling frameworks.

Compared to vector magnetisation inversion (MVI) techniques proposed by Lelièvre and Oldenburg (2009), which allow spatial variation of magnetisation but often suffer from instability in under-constrained scenarios, our approach assumes a uniform direction. It achieves consistent and interpretable results when remanence is strong and coherent.

The synthetic tests explicitly include noise, and the residual histograms (Fig. 8) summarise data fit across scenarios. The residuals exhibit a near-Gaussian distribution centred around zero, confirming that the inversion reproduced the observed data within an acceptable noise level. This, combined with the consistent performance across synthetic and real data, reinforces the proposed workflow's methodological reliability and practical applicability.

The histogram in Fig. 8 displays the residual distributions for the three synthetic models (A-C) and the real data (D). In all cases, the residuals are predominantly centred around zero, indicating good agreement between observed and predicted data. Model A (without remanence) presents the widest distribution, ranging from –20

to 20 nT, with most values tightly concentrated near zero (Fig. 8A). Model B (with incorrect magnetisation direction) shows a narrower range, from −1.5 to 1.5 nT, also centred near zero, indicating a smoother inversion fit despite the geometric inaccuracy (Fig. 8B). Model C (with estimated total magnetisation direction) ranges from −2 to 2 nT, with values slightly biased around 0.3 nT (Fig. 8C). The real dataset exhibits a broader spread, between −30 and 30 nT, yet remains centred around zero, corroborating the robustness and practical effectiveness of the proposed workflow under field conditions (Fig. 8D).

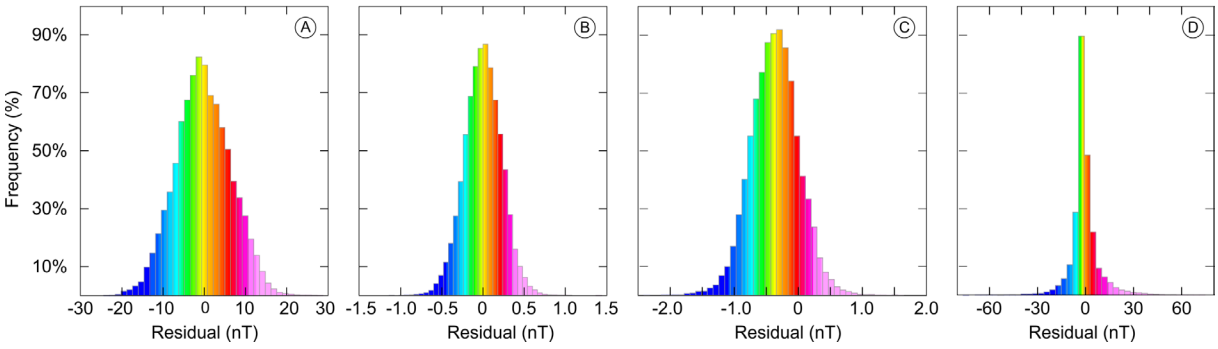

Figure 8. Histogram of residuals from the inversion results. (A) Model without remanent magnetisation; (B) Model with remanence using incorrect magnetisation direction; (C) Model with remanence using the estimated direction from the equivalent layer; (D) Real dataset. All distributions are approximately centred around zero. The broader spread observed in (B) and (D) reflects the misfit introduced by incorrect directional assumptions and the complexity of real data, respectively.

Acknowledging that the current methodology assumes a constant magnetisation direction within the source body is important. This may limit its applicability in complex geological settings involving multiple sources or internal variation of remanent direction. In such cases, further developments may involve combining this approach with MVI techniques to allow for spatial variation, or hybrid methodologies that adaptively apply EL-based direction estimation within locally homogeneous domains.

The susceptibility model recovered from the VOXI inversion reveals a moderately elongated magnetic body with a westward-dipping geometry and a variable depth range. This dip may partially explain the slight misalignment between the anomaly and the predicted field during the equivalent layer inversion, as the EL method assumes horizontal layering at a fixed depth. The isosurfaces in Fig. 7 represent susceptibility thresholds of 0.05, 0.10, 0.20, and 0.50 SI, with red volumes corresponding to lower susceptibility and blue to higher. A noticeable decrease in susceptibility values with increasing depth is observed, which may result from the smoothness-constrained inversion approach discussed previously in section 5.4. This depth-related gradient suggests that the inversion prioritised continuity and stability over sharp contrasts, potentially underestimating deeper concentrations. Despite this, the model remains coherent with the observed anomaly, validating the application of the proposed workflow to real datasets.

7. Conclusions

This study demonstrated the importance of accounting for remanent magnetisation in magnetic inversion workflows. Through a series of controlled synthetic tests and the application to real airborne magnetic data, we validated a sequential methodology that combines the estimation of the total magnetisation direction using the equivalent layer (EL) technique with traditional magnetic susceptibility inversion via the VOXI Earth Modelling system. The synthetic cases demonstrated that inversion produces distorted geometries and incorrect susceptibility estimates when the remanent direction is either ignored or incorrectly assumed.

Conversely, the geometry and susceptibility distribution closely resemble the true model when the remanent direction is accurately recovered. In the workflow, the inclination and declination estimated from the equivalent layer are used to perform a reduction to the pole (RTP), providing a corrected anomaly that serves as input for the VOXI inversion under the assumption of a vertical inducing field ($D = 0°, I = 90°$). This ensures that the susceptibility

model is derived from a magnetically centred dataset while maintaining a stable inversion framework. These results were further corroborated by applying real data from Espírito Santo (Brazil), where the method produced coherent susceptibility structures consistent with the observed magnetic anomaly.

The scientific contribution of this work lies in integrating two techniques that are often used independently: equivalent-layer-based estimation of magnetisation direction and traditional susceptibility inversion. Although conceptually simple, this sequential combination has not been systematically applied or validated in the presence of strong remanent magnetisation. The methodology proved effective under both idealised and field conditions, addressing key challenges such as data noise, direction estimation, and volumetric recovery of magnetic bodies. Compared with prior studies, such as those by Li et al. (2010), our approach offers a practical and stable alternative for cases where the magnetisation is coherent and approximately uniform.

However, it is important to note that the inversion strategy employed here assumes a constant magnetisation direction throughout the source body. While this assumption is reasonable for many geological settings, it may not hold in more complex scenarios involving multiple sources or internal heterogeneities. In such cases, inversion techniques that allow spatial variations in magnetisation direction, such as magnetisation Vector Inversion (MVI), may be required to capture the true structure and composition of the source. Future developments could explore hybrid strategies that combine the directional robustness of the equivalent layer method with the spatial flexibility of MVI or integrate probabilistic frameworks to quantify uncertainty in direction estimation and susceptibility recovery.

Overall, the study provides a reproducible workflow for remanence-affected magnetic interpretation: EL-based estimation of total magnetisation direction, RTP computed with that direction, and VOXI susceptibility inversion on the RTP dataset under a vertical inducing field. The synthetic tests and the Espírito Santo case study demonstrate that this sequence mitigates directional artefacts and yields more interpretable susceptibility models when remanence is spatially coherent.

References

Barbosa, R. D. L. (2021). Modelagem e inversão de dados potenciais da região do Parque dos Gaviões na Bacia do Parnaíba, Master's thesis, Universidade Federal Fluminense, https://app.uff.br/riuff/handle/1/27923.

Barbosa, V. C. F. and J. B. C. Silva (1994). Generalized compact gravity inversion, Geophysics, 59, 1, 57-68, doi:10.1190/1.1443534.

Blakely, R. J. (1995). Potential Theory in Gravity and Magnetic Applications, Cambridge University Press, Cambridge, 464, doi:10.1017/CBO9780511549816.

Brown, L. and S. McEnroe (2011). Remanent magnetism, in Encyclopedia of Solid Earth Geophysics, H. K. Gupta (Ed.), Springer, Dordrecht, 1024-1030, doi:10.1007/978-90-481-8702-7_126.

Cockett, R., S. Kang, L. J. Heagy, A. Pidlisecky et al. (2015). SimPEG: An open source framework for simulation and gradient based parameter estimation in geophysical applications, Comput. Geosci., 85, 142-154, doi:10.1016/j.cageo.2015.09.015.

Cunningham, M., C. Samson, J. Laliberté, M. Goldie et al. (2021). Inversion of magnetic data acquired with a rotary-wing unmanned aircraft system for gold exploration, Pure Appl. Geophys., 178, 1, 501-516, doi:10.1007/s00024-021-02664-8.

Dampney, C. N. G. (1969). The equivalent source technique, Geophysics, 34, 1, 39-53, doi:10.1190/1.1439996.

Dentith, M. and S. T. Mudge (2014). Geophysics for the Mineral Exploration Geoscientist, Cambridge University Press, Cambridge, 438, ISBN:978-0-521-80951-1.

Gonzalez, S .P., V. C. F. Barbosa and V. C. Oliveira (2020). Estimate of the remanent magnetisation direction via equivalent layer, in SEG Tech. Program Expanded Abstracts, 969-973, doi:10.1190/segam2020-3428268.1.

Gonzalez, S. P., V. C. F. Barbosa and V. C. Oliveira Jr. (2022). Analyzing the ambiguity of the remanent-magnetisation direction separated into induced and remanent magnetic sources, J. Geophys. Res. Solid Earth, 127, 12, e2022JB024151, doi:10.1029/2022JB024151.

Guevara-Betancourt, R., V. Yutsis, N. Varley, J. Almaguer et al. (2023). Insights into the plumbing system of Colima Volcanic Complex from geophysical evidence, J. Volcanol. Geotherm. Res., 433, 107711, doi:10.1016/j.jvolgeores.2022.107711.

Ingram, D. M., D. M. Causon and C. G. Mingham (2003). Developments in Cartesian cut cell methods, Math. Comput. Simul., 61, 3-6, 561-57, doi:10.1016/S0378-4754(02)00107-6.

Jian, X., S. Liu, X. Hu, Y. Zhang et al. (2022). A new method to estimate the total magnetisation direction from the magnetic anomaly: Multiple correlation, Geophysics, 87, 5, G115-G135, doi:10.1190/geo2021-0733.1.

Lelièvre, P. G. and D. W. Oldenburg (2009). A 3D total magnetisation inversion applicable when significant, complicated remanence is present, Geophysics, 74, 3, L21-L30, doi:10.1190/1.3103249.

Li, X. (2008). Magnetic reduction-to-the-pole at low latitudes: Observations and considerations, Lead. Edge, 27, 8, 990-1002, doi:10.1190/1.2967550.

Li, Y. and D. W. Oldenburg (1996). 3-D inversion of magnetic data, Geophysics, 61(2), 394-408.

Li, Y. and D. W. Oldenburg (2001). Stable reduction to the pole at the magnetic equator, Geophysics, 66, 2, 571-578, doi:10.1190/1.1444948.

Li, Y., S. E. Shearer, M. M. Haney and N. Dannemiller (2010). Comprehensive approaches to 3D inversion of magnetic data affected by remanent magnetisation, Geophysics, 75, 1, L1-L11, doi:10.1190/1.3294766.

Liu, S., X. Hu, D. Zhang, B. Wei et al. (2020a). The IDQ curve: A tool for evaluating the direction of remanent magnetisation from magnetic anomalies, Geophysics, 85, 3, J85-J98, doi:10.1190/geo2019-0545.1.

Liu, S., X. Hu, B. Zuo, H. Zhang et al. (2020b). Susceptibility and remanent magnetisation inversion of magnetic data with a priori information of the Köenigsberger ratio, Geophys. J. Int., 221, 2, 1090-1109, doi:10.1093/gji/ggaa057.

Luo, Y. and M. Wu (2023). Reduction to the pole near the equator with a Fourier-domain equivalent dipole layer, Geophysics, 88, 1, G115-G124, doi:10.1190/geo2022-0672.1.

MacLeod, I. N. and R. G. Ellis (2016). Quantitative magnetisation vector inversion, ASEG Extended Abstracts, 1-6, doi:10.1071/ASEG2016ab115.

Melo, F. F., S. P. Gonzalez, V. C. F. Barbosa and V. C. Oliveira Jr. (2021). Amplitude of the magnetic anomaly vector in the interpretation of total-field anomaly at low magnetic latitudes, J. Appl. Geophys., 190, 104339, doi:10.1016/j.jappgeo.2021.104339.

Milsom, J. and A. Eriksen (2011). Field Geophysics, 4th ed., Wiley, Hoboken, NJ, 265, ISBN:978-0-470-74984-5.

Nabighian, M. N. (1984). Toward a three-dimensional automatic interpretation of potential field data via generalized Hilbert transforms: Fundamental relations, Geophysics, 49, 6, 780-786, doi:10.1190/1.1441706.

Nagata, T. (1961). Rock Magnetism, Maruzen Co. Ltd., Tokyo, 350, doi:10.1017/S0016756800050573.

Nicolosi, I., I. Blanco-Montenegro, A. Pignatelli and M. Chiappini (2006). Estimating the magnetization direction of crustal structures by means of an equivalent source algorithm, Physics of the Earth and Planetary Interiors, 155, 3-4, 163-169, doi:10.1016/j.pepi.2005.12.003.

Pedrosa-Soares, A. C., C. M. Noce, C. Wiedemann and C. P. Pinto (2001). The Araçuaí-West-Congo Orogen in Brazil: An overview of a confined orogen formed during Gondwanaland assembly, Precambrian Res., 110, 1-4, 307-323, doi:10.1016/S0301-9268(01)00174-7.

Pilkington, M. (1997). 3-D magnetic imaging using conjugate gradients, Geophysics, 62, 4, 1132-1142, doi:10.1190/1.1826377.

Reeves, C. (2005). Aeromagnetic Surveys: Principles, Practice and Interpretation, Geosoft, Washington DC, 155.

Reis, A. L. A., V. C. Oliveira and V. C. F. Barbosa (2019). Equivalent layer technique for estimating magnetisation direction, in SEG Technical Program Expanded Abstracts 2019, 1769-1773, doi:10.1190/segam2019-3216745.1.

Reis, A. L. A., V. C. Oliveira, E. Yokoyama, A. C. Bruno et al. (2016). Estimating the magnetisation distribution within rectangular rock samples, Geochem. Geophys. Geosyst., 17, 8, 3350-3374, doi:10.1002/2016GC006329.

Reis, A. L. A., V. C. Oliveira Jr. and V. C. F. Barbosa (2020). Generalized positivity constraint on magnetic equivalent layers, Geophysics, 85, 3, J99-J110, doi:10.1190/geo2019-0706.1.

Schmidt, P. W. and M. A. Lackie (2014). Practical considerations: Making measurements of susceptibility, remanence and Q in the field, Explor. Geophys., 45, 4, 305-313, doi:10.1071/EG14019.

Sordi, D. A. D. (2021). Atlas aerogeofísico do estado do Espírito Santo, Geological Survey of Brazil, CPRM, http://rigeo.sgb.gov.br/jspui/handle/doc/22266.

Telford, W. M., R. E. Sheriff and L. P. Geldart (2003). Applied Geophysics, 2nd ed., Cambridge University Press, Cambridge, 770.

Tikhonov, A. N. (1963). Solution of incorrectly formulated problems and the regularization method, Sov. Math. Dokl., 4, 1035-1038.

Uhlein, A., J. R. Junior, M. Egydio-Silva, Y. M. Parizek-Silva et al. (2014). Geologia, petrologia e contexto geotectônico dos gnaisses e granitóides da região de Colatina, Espírito Santo, Geonomos, 22, 2, 166-181, doi:10.18285/geonomos.v22i1.295 .

Appendix. Inversion Parameter Detail

To evaluate the stability of the total-field inclination and declination estimated by the equivalent-layer (EL) approach, planar layers were constructed at five depths ranging from 100 m to 1000 m using the synthetic Model C (sphere test). The L2 norm of the misfit (Fig. A1) is lowest at 100 m, indicating the best agreement with the observed data. The total magnetisation directions for the shallower layers (100 m and 250 m) remain consistent, particularly in inclination, whereas the deeper layers (≥500 m) exhibit increasing discrepancies and deviate significantly from the shallow-layer solutions.

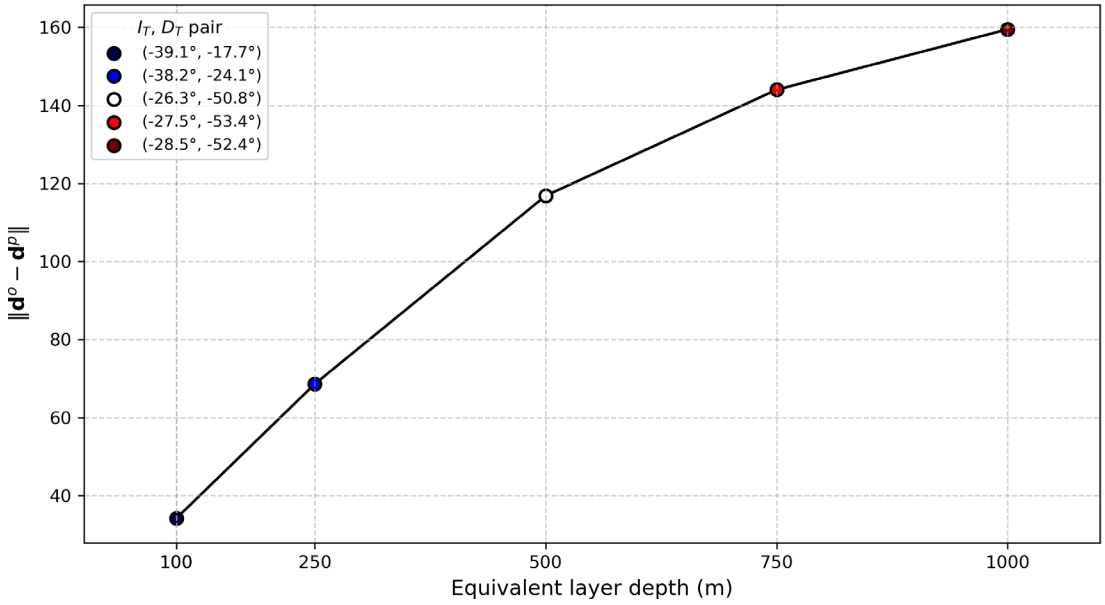

Figure A1. L_2 norm of the misfit as a function of equivalent-layer depth. Each marker represents a pair of estimated total-field inclination (I) and declination (D) for that depth. Blue tones correspond to shallower layers (100 m and 250 m), white to intermediate (500 m), and red to deeper (750 m and 1000 m).

The predicted total-field anomalies (Fig. A2), computed from the magnetic-moment intensities and the estimated total magnetisation directions under the positivity constraint, closely reproduce the simulated data at 100 m. Layers positioned at greater depths show larger differences between predicted and observed anomalies, confirming a progressive degradation of fit with increasing EL depth.

The reduced-to-the-pole (RTP) anomalies obtained using these estimates are displayed in Fig. A3. The shallower layers (100-250 m) produce centred, symmetric RTP anomalies, allowing a more precise delineation of the magnetic source, whereas deeper layers yield distorted, decentered patterns. As the estimates for the 100 m layer provided the best fit and the most stable directional solution, the pair (It = −39.1°, Dt = −17.7°) was adopted for the subsequent inversion.

The reduced-to-the-pole (RTP) anomalies obtained using these estimates are displayed in Fig. A3. The shallower layers (100-250 m) produce centred, symmetric RTP anomalies, allowing clearer delineation of the magnetic source, whereas deeper layers yield distorted, decentered patterns. As the estimates for the 100 m layer provided the best fit and the most stable directional solution, the pair (It = −39.1°, Dt = −17.7°) was adopted for the subsequent inversion.

The uncertainty bounds for (I, D) were inferred from the topology of the misfit surface in the inclination-declination space and from the directional variability across layers. Within the low-misfit region (100-250 m), inclination and declination vary smoothly, defining the practical confidence range of the EL solution. The dispersion of values around the minimum misfit corresponds to an uncertainty of approximately ±1° in inclination and ±6° in declination.

To quantify this variability, the total magnetisation direction within the stability range (100-250 m) was averaged, yielding It = −38.6° ± 0.5° and Dt = −20.9° ± 3.2°. These values represent realistic confidence bounds for the EL-based estimation and reflect the non-linear sensitivity of the (I, D) pair to equivalent-layer depth. They provide the required uncertainty estimates for the magnetisation direction used in the RTP correction and confirm the robustness of the adopted parameters.

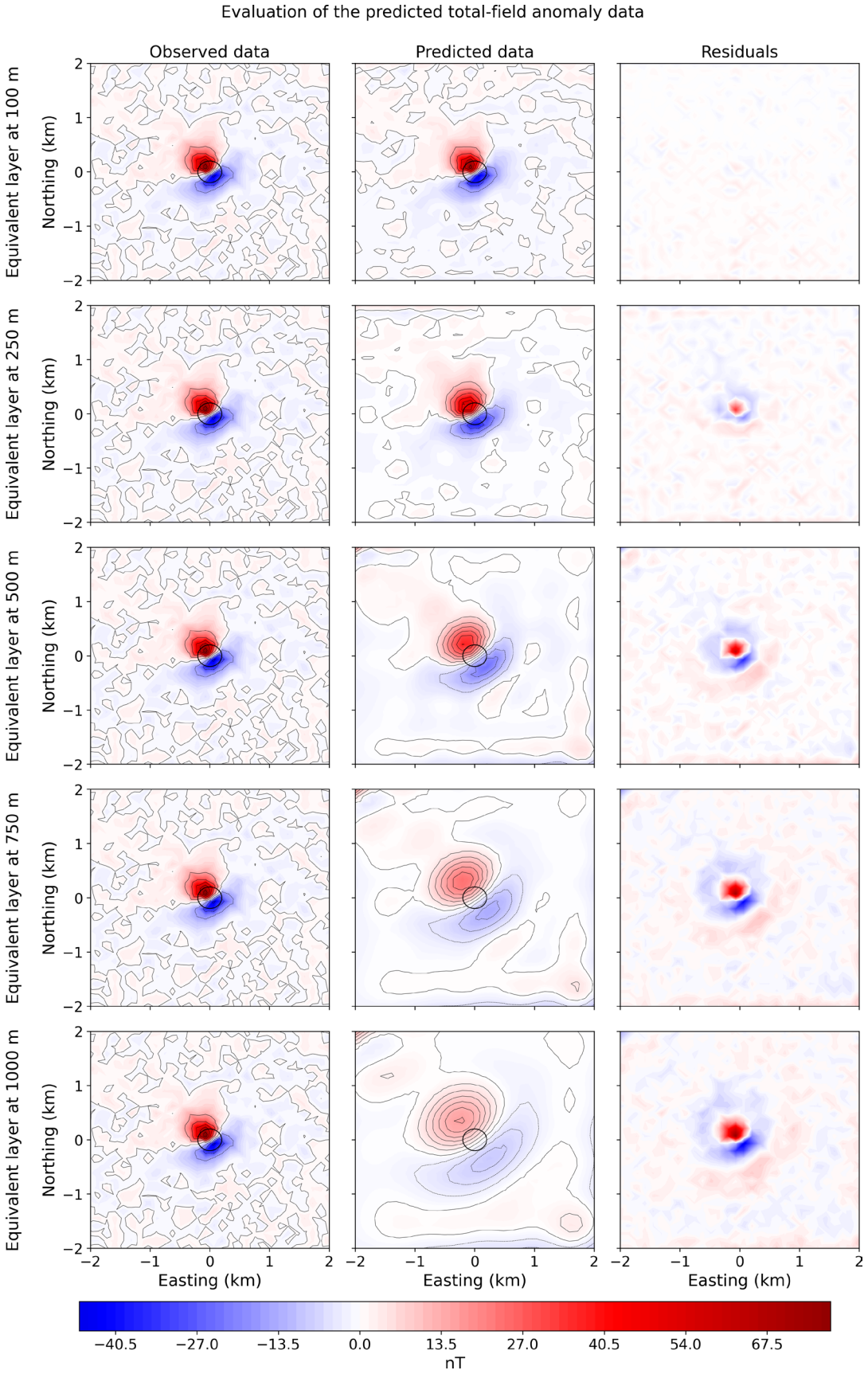

Figure A2. Observed and predicted total-field anomalies with residuals. Predictions were computed from magnetic-moment intensities and estimated total magnetisation directions, subject to the positivity constraint, for layers at different depths. Each row corresponds to a planar layer from 100 m to 1000 m. The black circle represents the projected outline of the modelled sphere.

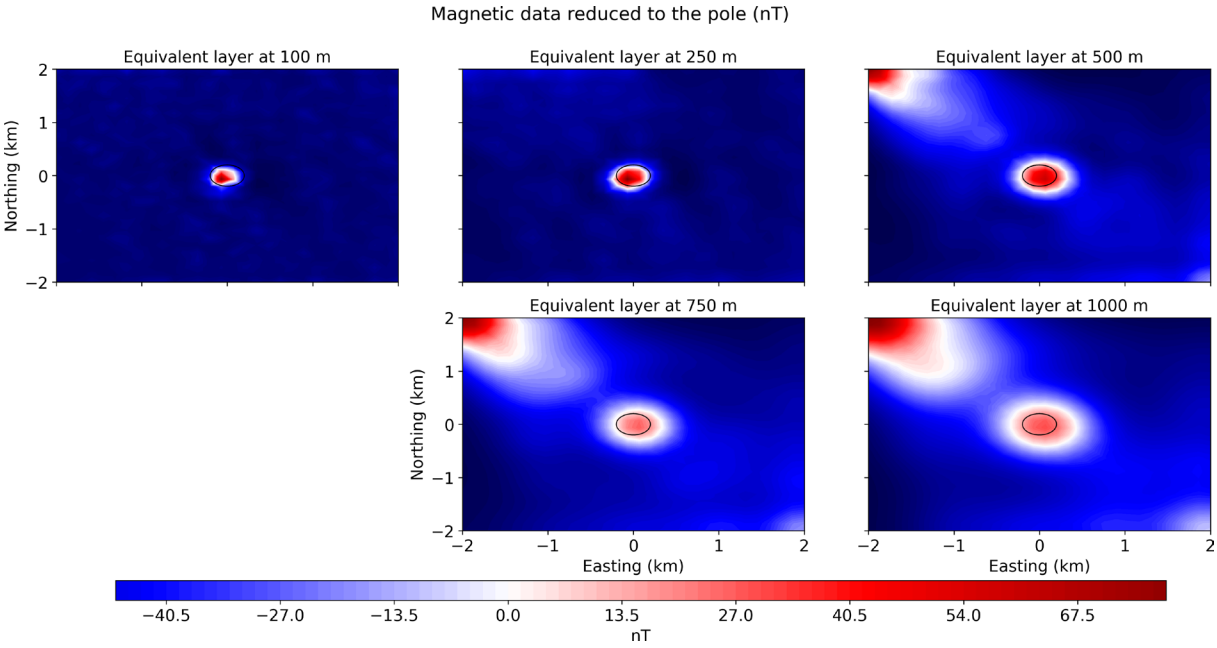

Figure A3. Total-field anomalies reduced to the pole (RTP) for layers between 100 m and 1000 m. Shallower layers produce centred and symmetric RTP anomalies, whereas deeper layers yield distorted and decentered patterns. The black circle indicates the projected outline of the modelled sphere.

***CORRESPONDING AUTHOR: Saulo S. MARTINS**,
Graduate Program in Geophysics, Universidade Federal do Pará, Campus Universitário,
R. Augusto Corrêa, 01 – Guamá, Belém, 66075-110, Pará, Brazil
e-mail: saulo@ufpa.br